

## Effect of High Frequency Current Injection on Optical Feedback Noise in Semiconductor Lasers Operating in Multimode

Sazzad MS Imran\*

Department of Applied Physics, Electronics & Communication Engineering, University of Dhaka, Bangladesh

### Abstract

The performance of semiconductor injection lasers is limited by optical feedback noise. The laser intensity noise is greatly increased even by small amount of optical feedback. Although superposition of high-frequency current on the injection current is popularly used to solve the problem, proper modulation frequency and depth must be chosen empirically. In this paper, we numerically analyze this problem based on a set of multimode rate equations, modified to include OFB (optical feedback) and HFI (high frequency current). We concentrate only on low frequency type noise where intensity noise is maximum in the lower frequency region. The results show that the feedback noise was reduced when HFI released coupling effects and thereby suppressed mode hopping. The feedback noise was still remained high when the modulation frequency was coincided with a rational number of the round trip time period of optical feedback. A simple formula together with a tree is newly reported from experimental and numerical data to find the rational numbers at which the feedback noise remains high for a particular external cavity length. Dependency of the rational numbers on external cavity lengths is also reported in this paper.

**Keywords:** Optical feedback noise; Semiconductor laser; Mode hopping; High frequency current; Intensity noise; Modulation

### Introduction

Semiconductor lasers play a central role in the growing world of optoelectronic technologies. A measure of the importance of this emerging optoelectronic technology is provided by the optical disc players and fiber optics communication system. Although these optical devices are already available commercially, several technological problems must be solved to further improve their performance. One such problem is the excess intensity noise called the Optical Feed Back (OFB) noise, which is induced by the re-injection of output light into the laser followed by reflection at surface of connecting optical device [1]. Experiments show that the RIN is increased by 20dB or more as a result of this external feedback [2]. The increase in RIN degrades the SNR and severely affects the performance of the system.

Intense research activity in recent years has been focused on the suppression of feedback-induced RIN enhancement of these lasers [3-5]. In a simple scheme known as the high-frequency injection technique, high-frequency current is superposed on laser driving current [6-8]. The experimental results show that the RIN increase does not occur if the modulation frequency and amplitude are suitably optimized [9]. The second method is the use of a self-pulsing laser, which is effective in reducing the excess noise due to mode competition among the external cavity modes [10,11]. The third method is the application of an electric negative feedback, which is effective for suppressing the quantum noise but not so effective for reducing the optical feedback noise [5,12].

Superposition of HF current is the most popularly used among them. Until now, mechanism of intensity noise reduction by HF superposition has been theoretically analyzed by some authors [3,5,8,12,13], though a profound understanding on some points has been still lacking. Sacher et al. reported on intensity instabilities of semiconductor lasers under current modulation in some ratios of driving modulation frequency and round-trip frequency [13]. Later, Yamada et al. reported on rising up of RIN when modulation frequency coincide a rational number of round-trip frequency [12]. They theoretically and analytically analyzed the problem taking into account only external cavity mode hopping, and did not mention about some specific rational numbers at which RIN values raised up.

In this paper, we present a self-contained numerical model that is capable of explaining RIN characteristics induced by external OFB and how this excess noise can be avoided through high-frequency current injection. Unlike previous analyses, we analytically and numerically analyzed the problem considering internal lasing mode hopping. We also report a simple formula to find out exact ratios of modulation frequency and round-trip frequency at which the RIN raised up for a particular external cavity length.

Our model is applied to 850-nm GaAs lasers, and characteristics of the OFB noise are expressed in terms of Relative Intensity Noise (RIN).

In the next section we present multimode rate equation model for analysis and basic equations of the model. In Sec. III, process of analysis and numerical calculation is explained. Sec. IV focuses on intensity noise characteristics due to external optical feedback, without application of high-frequency current, to understand the mechanism of noise generation. In Sec. V, mechanism and ability of noise reduction through high-frequency current injection are demonstrated. In Sec. VI, conclusions are given.

### The Rate Equation Model

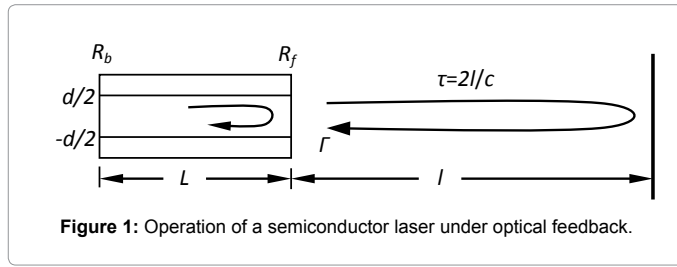
First it is to mention that we discuss here the model considering a stable laser in which only fundamental transverse mode exists. Figure 1 illustrates the operation of a semiconductor laser under optical feedback, where the external reflector is facing the low-reflectivity mirror. The cavity length and the effective refractive index of the laser are  $L$  and  $n_r$ , respectively. The distance between the laser and a reflecting mirror is  $l$ . The light emitted from the laser front facet is assumed to

\*Corresponding author: Sazzad MS Imran, Department of Applied Physics, Electronics & Communication Engineering, University of Dhaka, Bangladesh, Tel: 88 01817564087; E-mail: [sazzadmsi@du.ac.bd](mailto:sazzadmsi@du.ac.bd)

Received March 25, 2014; Accepted April 13, 2014; Published April 21, 2014

Citation: Imran SMS (2014) Effect of High Frequency Current Injection on Optical Feedback Noise in Semiconductor Lasers Operating in Multimode. J Laser Opt Photonics 1: 106. doi:10.4172/2469-410X.1000106

Copyright: © 2014 Imran SMS. This is an open-access article distributed under the terms of the Creative Commons Attribution License, which permits unrestricted use, distribution, and reproduction in any medium, provided the original author and source are credited.



travel single round-trip between the facet of reflectivity  $R_f$  and the external reflector with optical feedback ratio  $\Gamma$ , and then re-injects into the laser cavity. The round-trip time is  $\tau=2l/c$ , where  $c$  is the speed of light in vacuum.

Modal dynamics and noise characteristics of semiconductor lasers operating under external OFB can be studied by using time-delay rate equations of the modal photon number  $S_p(t)$ , modal phase  $\theta_p(t)$  and number of injected electrons  $N(t)$ . This model includes fluctuated spontaneous emission through a random term added to the rate equation for photon number and phase [1,14]. The effects of current modulation were also included in this model in a straightforward manner by generalizing the model. In general, these rate equations can be written as [15-18].

$$\frac{dS_p}{dt} = \left( G_p - G_{tho} + \frac{c}{n_r L} \ln |U_p| \right) S_p + \frac{a i N / V}{\left[ 2 \frac{(\lambda_p - \lambda_0)^2}{\delta \lambda} \right] + 1} + F_{sp}(t) \quad (1)$$

$$\frac{d\theta_p}{dt} = \frac{1}{2} \left[ \frac{\alpha a \xi}{V} (N - \bar{N}) - \frac{c}{n_r L} \right] + F_{\theta_p}(t) \quad (2)$$

$$\frac{dN}{dt} = - \sum_p A_p S_p - \frac{N}{\tau_s} + \frac{I}{e} \quad (3)$$

where  $G_p$  is the gain of mode  $p$  whose wavelength is  $\lambda_p$ ,  
 $G_{tho}$  is the threshold gain of the solitary laser.

$U_p$  is a function counting contribution of OFB to the instantaneous photon number  $S_p(t)$  of mode  $p$ .

These parameters are defined as

$$G_p = A_p - B_p S_p - \sum_{q \neq p} (D_{p(q)} + H_{p(q)}) S_q \quad (4)$$

$$G_{tho} = \frac{c}{n_r} \left[ k + \frac{1}{2L} \ln \frac{1}{R_f R_b} \right] \quad (5)$$

$$U_p = 1 - (1 - R_f) \sqrt{\frac{\eta \Gamma}{R_f}} \exp(-j\omega_p \tau) \sqrt{\frac{S_p(t-\tau)}{S_p(t)}} \exp(j\{\theta_p(t-\tau) - \theta_p(t)\}) = |U_p| \exp(-j\varphi) \quad (6)$$

$$\varphi = - \tan^{-1} \frac{\text{Im} U_p}{\text{Re} U_p} + m\pi \quad (-\pi \leq \varphi \leq \pi) \quad (7)$$

The Langevin noise sources  $F_{sp}(t)$  and  $F_{\theta_p}(t)$  are functions in inducing instantaneous fluctuations on photon number and phase due to spontaneous emission and the process of recombination. These are well approximated as Gaussian distributions with zero mean values and are given by [18]

$$F_p(t) = \sqrt{\frac{V S_p S_p}{\Delta t}} g_s \quad (8)$$

$$F_{\theta_p}(t) = \sqrt{\frac{V S_p S_p}{\Delta t}} \cdot \frac{g_\theta}{2(S_p + 1)} \quad (9)$$

Here,  $K_\alpha = (1 - R_f) \sqrt{\frac{\eta \Gamma}{R_f}}$  is a coefficient measuring the OFB strength.

$$V S_p S_p = \left[ \frac{a \xi}{V} (N + N_g) + G_{tho} \right] S_p + \frac{a \xi N}{V} \quad (10)$$

$A_p$  is the linear gain,  $B_p$  is the coefficient of self-suppression, and  $D_{p(q)}$  and  $H_{p(q)}$  are the coefficients of SGS and AGS, respectively. These coefficients are given by [16]

$$A_p = \frac{a \xi}{V} [N - N_g - bV(\lambda_p - \lambda_0)^2] \quad (11)$$

$$B_p = \frac{9}{4} \frac{\hbar \omega}{\epsilon_0 n_r^2} \left( \frac{\xi \tau_{in}}{\hbar V} \right)^2 a R_{cv}^2 (N - N_s) \quad (12)$$

$$D_{p(q)} = \frac{4}{3} \frac{B_p}{\left( \frac{2\pi c \tau_n}{\lambda_p^2} \right)^2 (\lambda_p - \lambda_q)^2 + 1} \quad (13)$$

$$H_{p(q)} = \frac{3\lambda_p^2}{8\pi c} \left( \frac{a \xi}{V} \right)^2 \frac{\alpha (N - N_g)}{\lambda_q - \lambda_p} \quad (14)$$

We have neglected noise source on the electron extinction in this model as this has less affects in calculated results than those for the photon generation [18]. The electron number  $N(t)$  suffers sufficient fluctuation from the Langevin noise sources  $F_p(t)$  through (1), (2) and (11).

In (1),  $a$  is the differential gain coefficient,  $\xi$  is the field confinement factor,  $V$  is the volume of the active region,  $\lambda_0$  is the peak wavelength and  $\delta \lambda$  is the half-width of spontaneous emission. In (2)  $\alpha$  is the linewidth enhancement factor and  $N_{bar} = \bar{N}$  is the time average value of  $N(t)$ . In (3)  $\tau_s$  is the electron lifetime,  $I$  is the injection current and  $e$  is the electron charge. In (5)  $k$  is the internal loss in the laser cavity. In (6)  $\eta$  is the coupling coefficient into the active region,  $\Gamma$  is the optical feedback ratio to the laser cavity,  $\omega_p = 2\pi c / \lambda_p$  is the angular frequency of mode  $p$ ,  $\omega_p \tau$  is the phase delay of the field in each roundtrip time. Here we assume  $\eta$  to be mode independent since the coupling efficiency is nearly the same for all longitudinal modes of the laser [3].

In (8) and (9)  $g_s$  and  $g_\theta$  are random number generations in ranges of [16,18]

$$-1 \leq g_s \leq 1 \text{ and } -1 \leq g_\theta \leq 1$$

and  $\Delta t$  is the time-step of the calculation. In (10)-(14),  $N_g$  is the electron number at transparency,  $b$  is the width of the linear gain coefficient,  $\hbar$  is the reduced Planck constant,  $\omega = 2\pi c / \lambda_0$  is the central angular frequency,  $\tau_n$  is the intraband relaxation time,  $R_{cv}$  is the dipole moment and  $N_s$  is the electron number characterizing the self-suppression coefficient.

The central mode,  $p=0$  with wavelength  $\lambda_0$ , is assumed to lie at the centre of the spectrum of gain. The wavelength of the other modes can be written as

$$\lambda_p = \lambda_0 + p\Delta\lambda = \lambda_0 + p \frac{\lambda_0^2}{2n_r L} \quad p = 0, \pm 1, \pm 2, \pm 3, \dots \quad (15)$$

Symbol	Definition	Value	Unit
$a$	tangential gain coefficient	$2.75 \times 10^{-12}$	$\text{m}^3\text{s}^{-1}$
$b$	dispersion parameter of the linear gain spectrum	$3 \times 10^{19}$	$\text{m}^3\text{A}^{-2}$
$ R_{\text{ex}} ^2$	squared absolute value of the dipole moment	$2.8 \times 10^{-57}$	$\text{C}^2\text{m}^2$
$\delta\lambda$	half-width of spontaneous emission	23	nm
$\alpha$	linewidth enhancement factor	2.6	-
$\xi$	confinement factor of field	0.2	-
$\tau_n$	electron intraband relaxation time	0.1	ps
$\tau_s$	average electron lifetime	2.79	ns
$N_s$	electron number characterizing non-linear gain	$1.7 \times 10^8$	-
$N_g$	electron number at transparency	$2.1 \times 10^8$	-
$V$	volume of the laser active region	100	$\mu\text{m}^3$
$d$	thickness of the laser active region	0.11	$\mu\text{m}$
$L$	length of the laser active region	300	$\mu\text{m}$
$n_r$	refractive index of laser active region	3.6	-
$k$	internal loss in the laser cavity	10	$\text{cm}^{-1}$
$R_f$	reflectivity of front facet	0.3	-
$R_b$	reflectivity of back facet	0.6	-

**Table 1:** Typical parameter values used in numerical simulations for 850-nm GaAs semiconductor laser.

where  $\lambda_0^2/(2n_r L)$  is the longitudinal-mode spacing of solitary laser.

The effect of high-frequency injection is included by modulating the injection current periodically with a modulation frequency  $f_M$ . The pumping term  $I$  in equation (3) then has to be replaced by

$$I = I_D + I_M \cos(2\pi f_M t) \quad (16)$$

where  $I_D$  is the bias current,  $I_M$  is the modulation current and  $f_M$  is the frequency of sinusoidal modulation.

The rate equations (1)-(3) can be used to obtain the RIN of the diode laser for the modulated signal in the presence of optical feedback by integrating them numerically and calculating the spectrum of intensity fluctuations.

It is to mention that in experiment, the individual modes are not distinguished. Rather, the system performance is governed by the total photon number [3]. The RIN for the total photon number is therefore given by

$$RIN = \frac{\langle S_\Omega^2 \rangle}{|S_M|^2} \quad (17)$$

where  $S_\Omega$  is calculated from the fluctuations  $\delta S(t) = S(t) - S_M(t)$  of the total photon number  $S(t) = \sum_p S_p(t)$  and  $S_M(t)$  is the modulating signal.

The values of intensity fluctuation for modulated signal is then computed in terms of RIN by employing the fast Fourier transform to integrate the discrete version of equation (17) as

$$RIN = \frac{1}{|S_M|^2} \frac{\Delta t^2}{T} |FFT[\delta S(t_i)]|^2 \quad (18)$$

Finally, we want to point out that the model used here to analyze laser actually is of great practical relevance since spurious feedback, as it occurs when coupling a laser diode to a fiber or in optical disc systems, corresponds to the situation considered here. This configuration can be considered as a delayed feedback of laser emission, back into the active region of the laser. Therefore,  $S_p(t-\tau)$  and  $\theta_p(t-\tau)$  considered in equation (6) are function of the photon number  $S_p(t)$  and phase  $\theta_p(t)$ , respectively, delayed by time  $\tau$  corresponding to the round-trip time in the external resonator [19].

We now describe the corresponding numerical procedure that has been followed before we discuss our results in sections IV and V in detail.

### Numerical calculation

The proposed model is applied in 850-nm GaAs lasers to investigate the effect of high-frequency modulation current on the characteristics of intensity noise caused by external optical feedback. We include thirteen longitudinal modes in our numerical simulations, which are performed using fourth-order Runge-Kutta algorithm to solve the rate equations (1)-(3) [20]. Time-step of integration is set as short as  $\Delta t = 5\text{ps}$ . This short time step corresponds to a cutoff Fourier frequency of 100GHz that is high enough to guarantee fine resolution of the OFB induced dynamics. The length of the external cavity was set between  $l = 15\text{cm}$  and  $l = 2.7\text{cm}$ , and the refractive index  $n_{\text{ex}} = 1$ . For the coupling constant we have used  $\eta = 0.02$  to estimate the optical feedback ratio  $\Gamma$ .

The integration is first made without OFB for solitary laser from time  $t=0$  until the round-trip time  $t=\tau$ . The calculated values of  $S_p(t=0 \rightarrow \tau)$  and  $\theta_p(t=0 \rightarrow \tau)$  of mode  $p$  are then stored for use as time delayed values  $S_p(t-\tau)$  and  $\theta_p(t-\tau)$ , including OFB terms, for the rest of the calculations. The dynamic states are examined after  $0.5 \mu\text{s}$ , which is long enough for the transients to be died out. The integration is then proceeded over a long period of time  $T = 2 \mu\text{s}$ . This time limit ensures computation of noise as low as 500 kHz. RIN is then computed directly from the obtained values of  $S(t) = \sum_p S_p(t)$  by employing the FFT to integrate equation (18).

Note that noise on the calculated RIN spectrum is due to the finite duration of computed time-resolved signal due to our impossibility to simulate infinitely long laser outputs. The RIN spectra are averaged over several trajectories to improve numerical accuracy [21]. The spectra are then smoothed by running an adjacent averaging of spectral components. The numerical values of 850-nm GaAs laser parameters, listed in Table 1, are employed in the calculations.

### Effect of optical feedback on laser dynamics

As mentioned in the introduction, it is useful to consider first the results describing RIN characteristics of semiconductor lasers operating in multimode in the presence of OFB. Optical feedback affects the noise

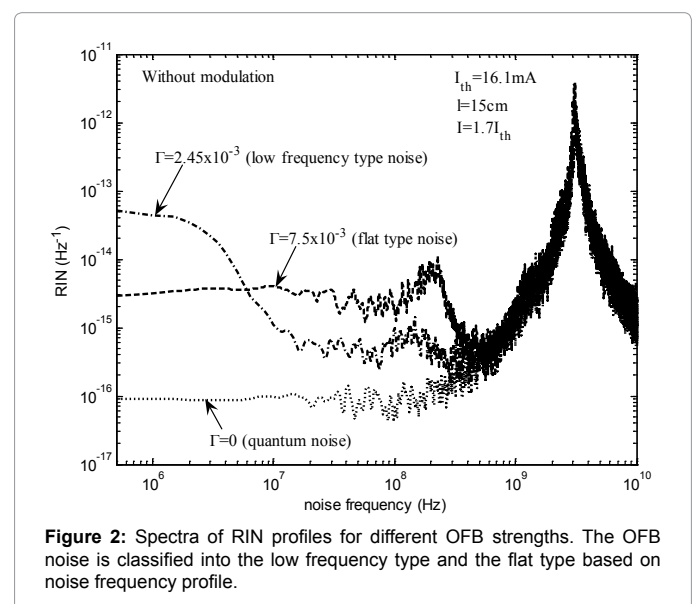


**Figure 2:** Spectra of RIN profiles for different OFB strengths. The OFB noise is classified into the low frequency type and the flat type based on noise frequency profile.

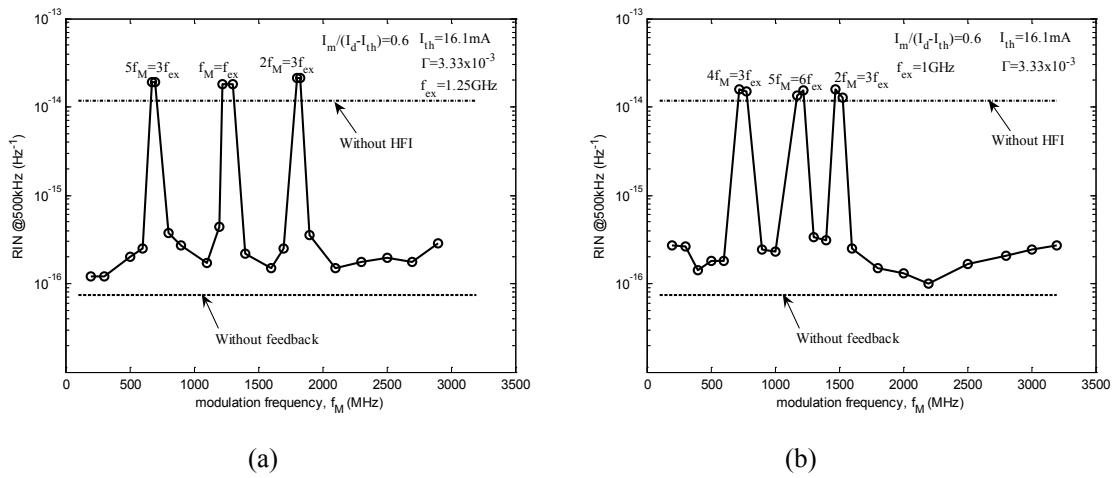


**Figure 3:** Dependence of low-frequency RIN on HFI modulation frequency for the OFB strength corresponds to low frequency type noise. (a) Numerical data for  $f_{ex} = 1.25\text{GHz}$  corresponding to  $l = 12\text{cm}$ , (b) Numerical data for  $f_{ex} = 1\text{GHz}$  corresponding to  $l = 15\text{cm}$ .

and dynamics of the laser in different ways, depending on the strength of external feedback. These different effects can be divided into two regimes of feedback as shown in Figure 2 for a typical 850-nm GaAs laser [2,22]. The RIN without feedback has a low value (approximately  $10^{-16} \text{ Hz}^{-1}$ ) for frequencies below 500MHz which corresponds to the quantum noise; and shows a broad peak near 3 GHz which corresponds to the relaxation-oscillation frequency. The RIN in lower frequency region of the spectrum ( $< 2 \text{ MHz}$ ) appeared to be enhanced by a large amount ( $> 20\text{dB}$ ) when the optical feedback ratio  $\Gamma$  was increased from 0 to  $2.45 \times 10^{-3}$ . This RIN enhancement is due to unstable mode hopping between bi-stable states of two longitudinal lasing modes [22]. We call here this type of noise to be low frequency type noise. When OFB ratio was increased more, the RIN profile became flat for wide frequency range from very low frequency to several 100MHz. We call here this type of noise to be flat type noise. This flat-type noise is independent of mode hopping between lasing modes [22] and generated due to mode competition among external modes whose lasing frequency is decided by the space between laser front facet and reflecting mirror [2].

In the next section we have discussed reduction of intensity noise, specifically the low frequency type noise, generated due to optical feedback by modulating laser injection current, a technique known as High-Frequency Injection (HFI).

### Control of laser RIN by HFI

As discussed in the preceding section, the primary problem caused by OFB in an optical system is the increase of laser intensity noise, particularly in the low frequency region. The ultimate goal of the high frequency current injection is to make the laser intensity noise resilient to changes in OFB. There have been different interpretations of the method by which HFI achieves this.

First opinion is that, HFI works because the time the feedback returns to the laser the modulation has turned the laser off [7]. This implies that some modulation frequencies will work better than others. Second interpretation is that, HFI changes a laser operating in bi-stable mode into a stable multimode laser [6], thus reduces the noise. Yamada and Higashi [8], on the other hand, argue that HFI acts to weaken the mode competition and thus effective as it suppresses mode hopping, not because a multimode laser is produced.

The point of view adopted in this paper, based on the experimental and theoretical analysis in [22], is that laser intensity noise increases for the low frequency type because of mode hopping between bi-stable lasing modes. For HFI to be effective, it must suppress the competition between the modes. Two parameters that are user controllable to achieve this are the modulation frequency and the depth of modulation.

We calculated RIN at 500kHz as a function of HFI modulation frequency for OFB strength corresponds to the low frequency type noise and the numerical results are shown in Figure 3. We also compare here the experimental results reported in (Figure 2 of ref. [12]) by Yamada et al. for  $f_{ex} = 700 \text{ MHz}$  corresponding to  $l = 21.5 \text{ cm}$  that shows increase of RIN at 700 MHz and 1150 MHz. From these obtained results, two regimes can be distinguished: (1) modulation frequency is of the same order of relaxation oscillation frequency, and (2) modulation frequency amounts to a rational fraction  $m/n$  of round-trip frequency. Simulations predict that modulating with a frequency near 200 MHz to relaxation oscillation frequency would serve to pin the laser noise to a low value. However, the RIN was increased or remained high when modulation frequency  $f_M$  of the superposed current coincided with a rational number of the round trip time period  $f_{ex}$ . This behavior is modeled by a very simple mathematical formula given below.

The RIN was increased or remained high when  $mf_M = mf_{ex}$  where  $m = 1, 3, 6, 9, \dots$  and  $n = 1, 2, 3, \dots$

This can also be formulated as

$$n(t) = n(t-1) + 1$$

$$m(t) = m(t-1) + 2 \quad \text{if } m(t-1) = 1$$

$$= m(t-1) + 3 \quad \text{if } m(t-1) \neq 1.$$

This formula predicts every rational number  $m/n$  corresponds to our frequency ratio  $f_M/f_{ex}$  where the RIN was increased. The predictions according to the formula have been checked numerically (Figure 3a and 3b) as well as experimentally (in Figure 2 of ref. [12]) for different  $f_{ex}$  values by changing the length of the external cavity. The numerical results shown in Figure 3 and experimental results reported in [12] are comparable qualitatively. Quantitative comparison between them is not easy, because we need to examine accurately the modulation current flowed into the active region instead of the applied HF power, the

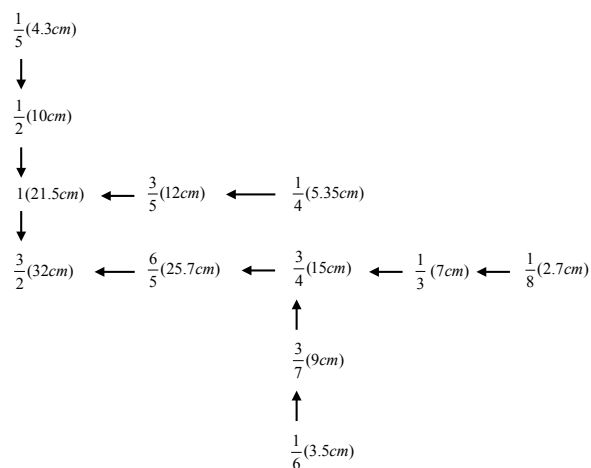


**Figure 4:** Observed ratios of the modulation frequencies to the round-trip frequencies where RIN was increased. The value in the parentheses corresponds to the external cavity lengths.

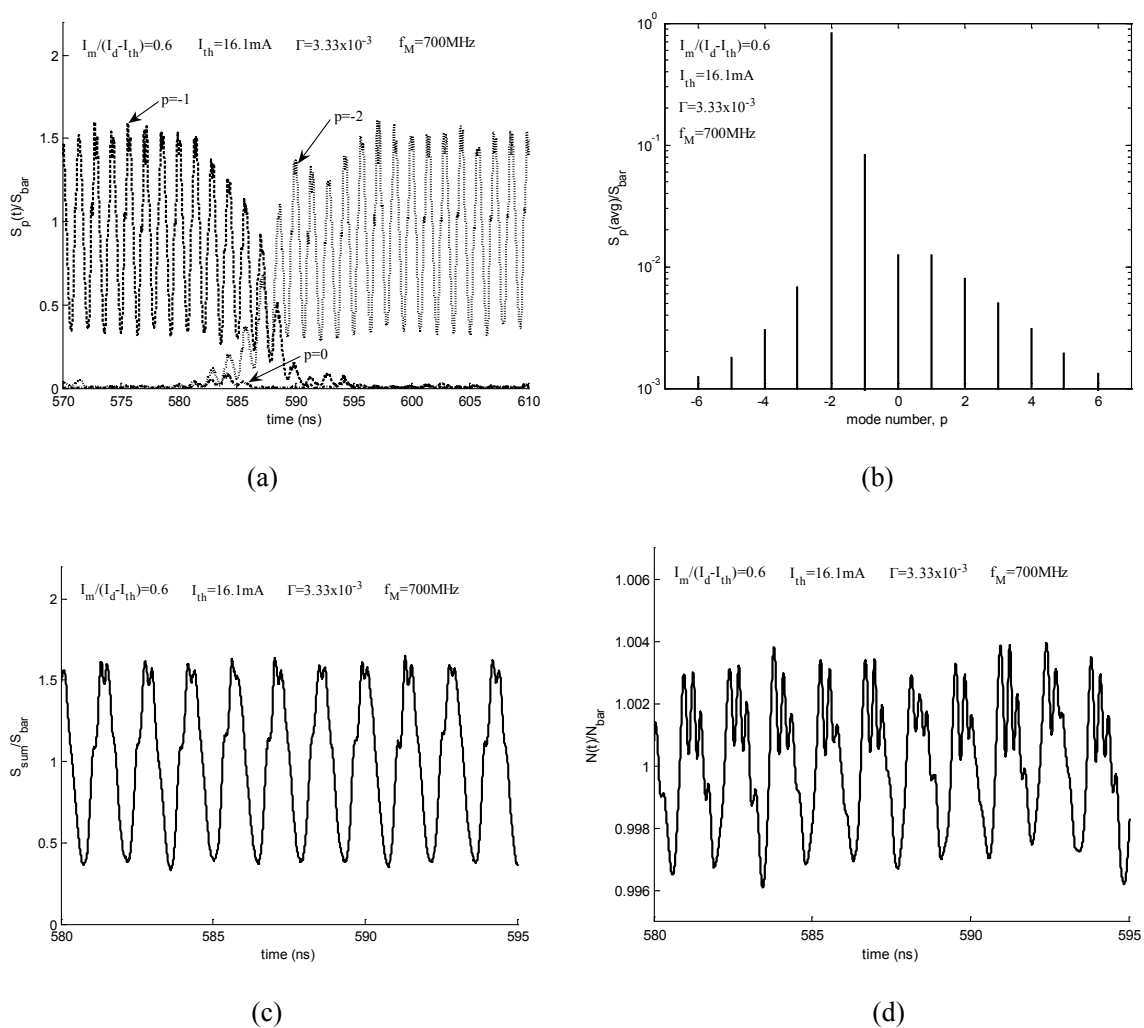


**Figure 5:** Modal behavior when the modulation frequency is a rational fraction of the round-trip frequency. (a) Temporal variation of all lasing modes, (b) Time-averaged modal spectrum, (c) Temporal variation of total lasing modes, (d) Temporal variation of carrier numbers. Here  $S_{bar} = \bar{S}$  is the time average value of photon number  $S(t)$  and  $S_{sum} = \sum_p S_p(t)$  is the total photon number.

coupling coefficient  $\eta$  for the optical feedback and fluctuation of optical feedback ratio to the laser cavity  $\Gamma$  with fluctuation of optical phase on the feedbacked light [12]. The observed ratios at which RIN remained high can be predicted from the tree in Figure 4.

The tree works as follows. When the external cavity length is 15 cm, the ratios  $f_M/f_{ex}$  where the RIN values were increased are  $3/4 \rightarrow 6/5 \rightarrow 3/2$  as found in Figure 3a. Similarly, for external cavity length of 12 cm the

ratios are  $3/5 \rightarrow 1 \rightarrow 3/2$  (Figure 3(b)) and for external cavity length of 21.5 cm the ratios are  $1 \rightarrow 3/2$  (Figure 2 in ref. [12]). In the same way, for external cavity length of 3.5 cm the ratios at which the RIN value will be higher are  $1/63/7 \rightarrow 3/4 \rightarrow 6/5 \rightarrow 3/2$ . Using the same formula and tree particular ratios  $f_M/f_{ex}$  can be predicted for any distance between laser output facet and external reflector.

Figure 5 shows modal behavior of the laser when modulation

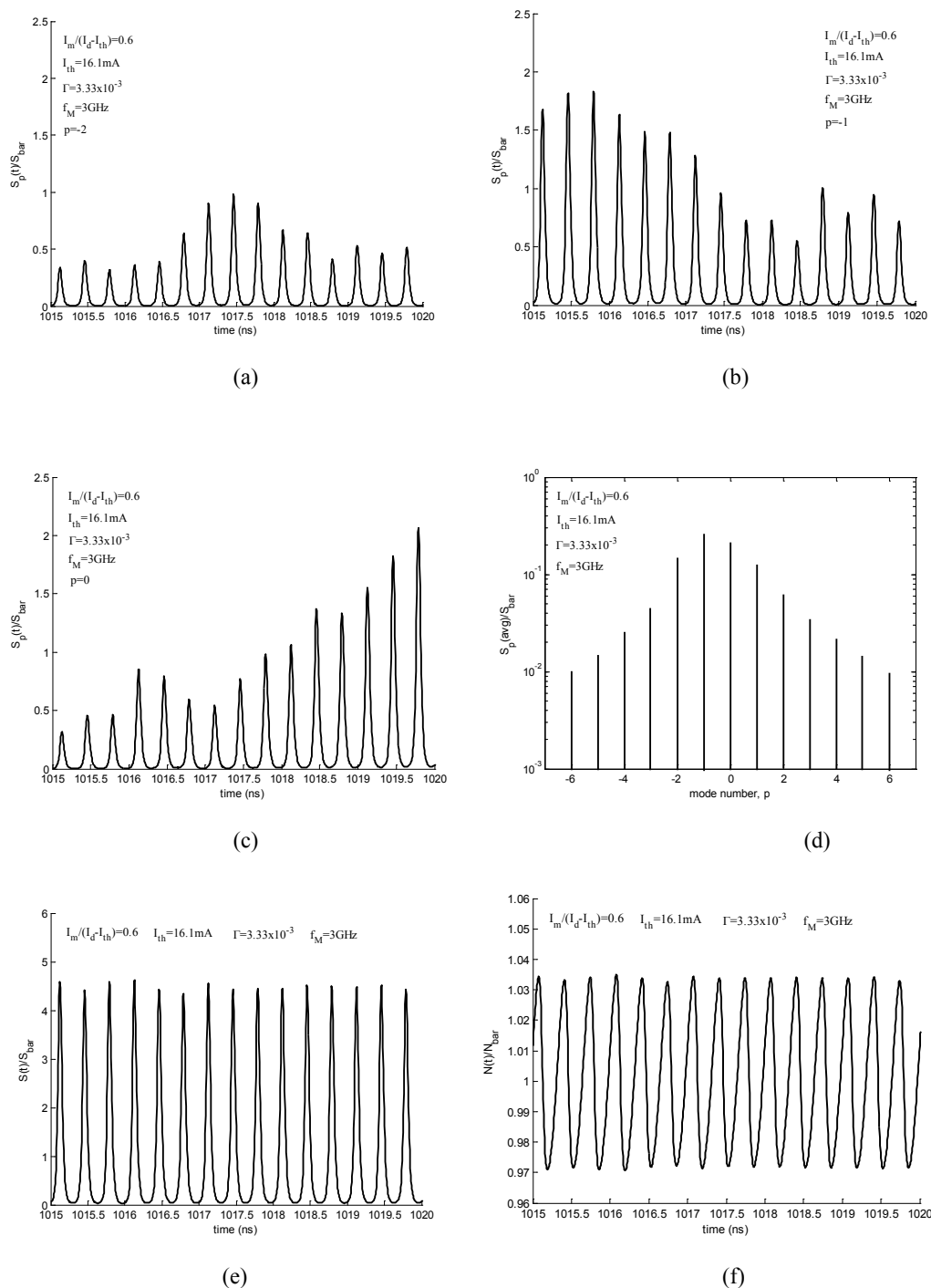


**Figure 6:** Modal behavior when modulation frequency is of the order of relaxation oscillation frequency. (a) Temporal variation of lasing mode -2, (b) Temporal variation of lasing mode -1, (c) Temporal variation of lasing mode 0, (d) Time-averaged modal spectrum, (e) Temporal variation of total lasing modes, (f) Temporal variation of carrier numbers.

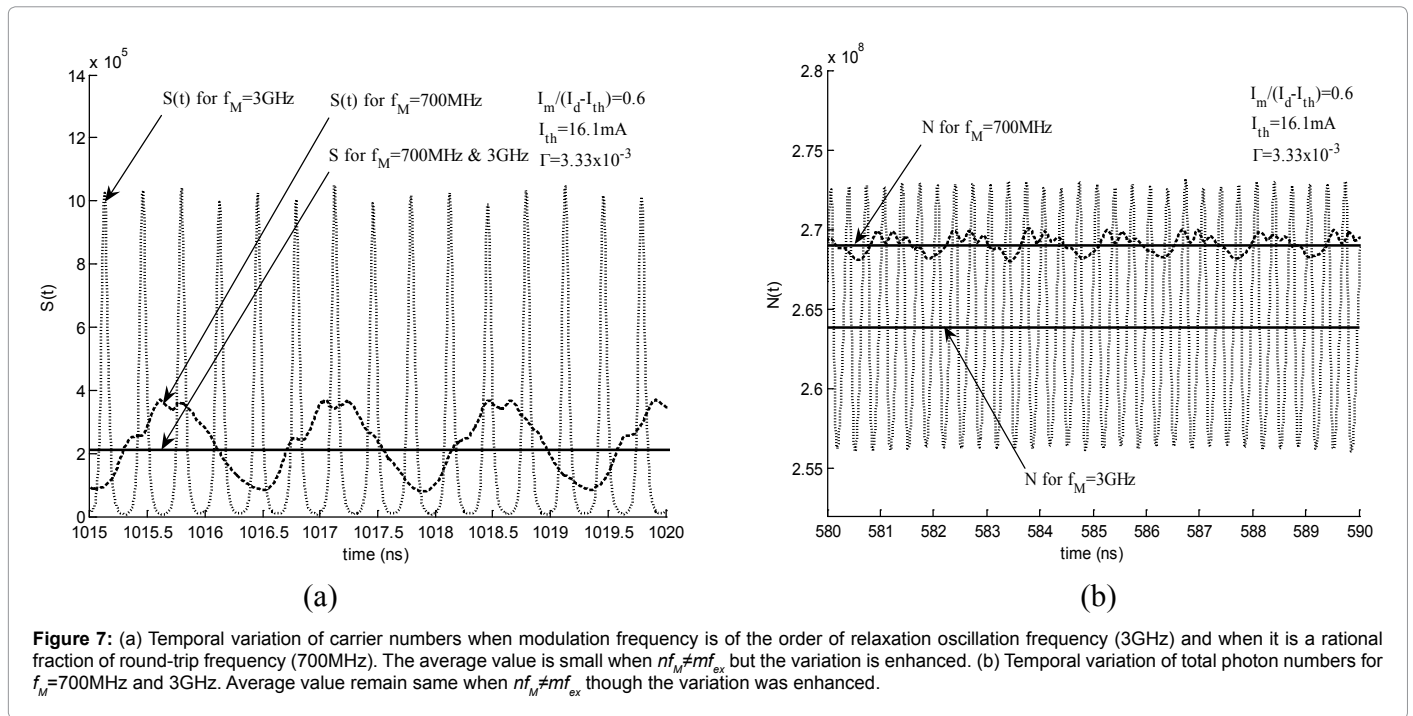


**Figure 7:** (a) Temporal variation of carrier numbers when modulation frequency is of the order of relaxation oscillation frequency (3GHz) and when it is a rational fraction of round-trip frequency (700MHz). The average value is small when  $nf_M \neq mf_{ex}$ , but the variation is enhanced. (b) Temporal variation of total photon numbers for  $f_M=700\text{MHz}$  and 3GHz. Average value remain same when  $nf_M \neq mf_{ex}$  though the variation was enhanced.

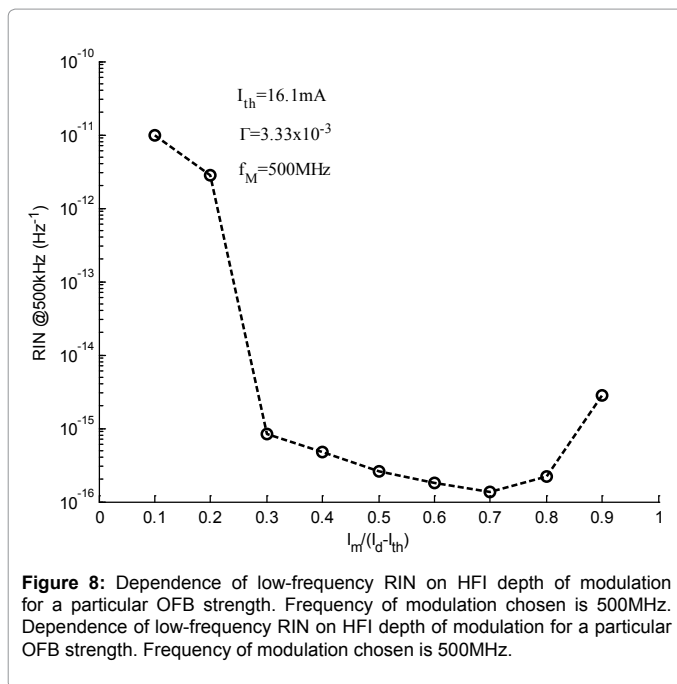


**Figure 8:** Dependence of low-frequency RIN on HFI depth of modulation for a particular OFB strength. Frequency of modulation chosen is 500MHz. Dependence of low-frequency RIN on HFI depth of modulation for a particular OFB strength. Frequency of modulation chosen is 500MHz.

frequency is a rational fraction of round-trip frequency, that is,  $f_M/f_{ex}=3/4$ . We have found that the laser exhibits mode hopping at random times between bi-stable states. Figure 5a and 5b confirm the mode hopping between two dominant modes  $p=-1$  and  $-2$ . We can say that due to this mode hopping, the RIN remained high in the lower frequency region.

When the HFI with modulation frequency near relaxation oscillation frequency was used, the simulation results in Figure 6, demonstrated that the laser now operated in multimode without any mode hopping being occurred. Individual lasing modes as well as

total mode exhibit pulsation at modulation frequency. Furthermore, oscillation amplitude of individual modes varies randomly from cycle to cycle, whereas that of total mode remains nearly constant. Physically, the mode powers grow by spontaneous emission when the laser goes below threshold during each cycle, and all modes have equal probability of being excited. Thus, amplitude of individual lasing mode fluctuates, even though the amplitude of total mode is nearly constant from cycle to cycle (Figure 6e). In this case, due to the absence of any mode hopping the low-frequency RIN value dropped to near quantum level.

From Figure 7 it is clear that the average value of injected carrier numbers became smaller when the modulation frequency is of the order of relaxation oscillation frequency ( $nf_M \neq mf_{ex}$ ) than when the modulation frequency is a rational fraction of round-trip frequency ( $nf_M = mf_{ex}$ ). This in turn enhanced variations of the injected electrons and photon numbers by almost 10 folds, though the average photon numbers remained same for both cases. The coupling effect among the longitudinal modes are released because of this enhanced vibration of the injected electron and larger variation of the gain [8], resulting in reduction of mode hopping noise when  $f_M/f_{ex} \neq m/n$ . This phenomenon was explained analytically in Appendix A.

However, it is undesirable to modulate injection current with relaxation oscillation frequency as it is difficult to generate such high frequency current of 3 GHz in practice. Also, modulation near relaxation oscillation frequency can destabilize the lasers with relatively short external cavities for which  $f_{ex} > f_{res}$  [3]. Therefore, we consider the optimum modulation frequency of 500 MHz for our numerical simulations. This is because at this frequency the laser exhibits similar RIN characteristics like relaxation oscillation frequency as the higher harmonics of this frequency coincides with  $f_{res}$ .

Figure 8 demonstrates the importance of the depth of modulation for HFI technique. It shows the RIN as a function of modulation current  $I_M$  when the modulation frequency is chosen to be 500 MHz. The lowest values of RIN occur for relatively large values of  $I_M$  such that the laser is driven below threshold over a part of the modulation cycle. Numerical

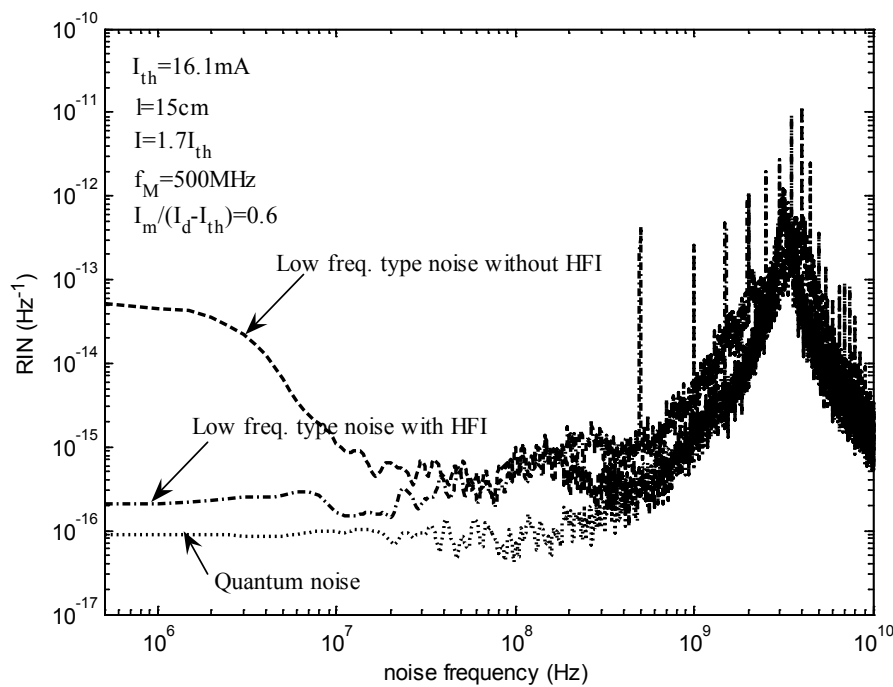


Figure 9: The simulated spectra of RIN profiles for low frequency type noise with HFI. Quantum noise spectra are also shown for comparison.

simulations indicate that mode switching is eliminated by the current modulation with larger  $I_M$  values.

For HFI to be effective, it must suppress the competition between the modes so that the RIN remains near the quantum noise level. Figure 9 demonstrates this effectiveness which shows the spectra of RIN profiles at feedback strength  $\Gamma = 2.45 \times 10^{-3}$  representing the low frequency type noise when the injection current is modulated at 500MHz with optimum modulation depth chosen from Figure 8 [23].

## Conclusion

Semiconductor lasers while in operation suffer from unwanted reflections that are fed back into the laser. Such optical feedback destabilizes the laser intensity leading to an increase in intensity noise. We have numerically integrated a well established model to study the effects of HFI on the dynamics of a multimode semiconductor lasers subject to optical feedback. We have centered our investigation on the feedback strength at which the laser shows low frequency type noise.

We have found that OFB in multimode laser, in the low frequency type region, forces the laser to hop between bi-stable modes and the laser exhibits an enhancement of low-frequency RIN. A solution to this problem was provided by modulation of the injection current at relatively high frequencies. But the modulation frequency that coincided with a rational number of the round-trip frequency for optical feedback must be avoided as the feedback noise was still remained high in this frequency. The rational numbers at which the RIN remained high was found to be dependent on external cavity lengths. A new formula together with a tree was given to easily find that rational numbers for a particular cavity length. Such characteristics were well explained analytically supported by numerical and experimental data.

The effectiveness of the HFI technique rests in its ability to suppress the mode competitions among the lasing modes. With proper choice of frequency and depth of modulation, the increase in RIN can be avoided.

## Acknowledgement

The author would like to thank Professor Minoru Yamada of Kanazawa University of Japan for his significant help to solve and understand the rate equations for semiconductor lasers.

## References

- Petermann K (1991) Laser Diode Modulation and Noise Boston MA: Kluwer.
- Yamada M, Kanamori A, Takayama S (1996) Experimental evidence of mode competition phenomena on the feedback induced noise in semiconductor lasers. IEICE Transactions on Electron E79-C: 1766-1768.
- Ryan AT, Agrawal GP, Gray GR, Gage EC (1994) Optical-feedback-induced chaos and its control in multimode semiconductor lasers. IEEE Journal of Quantum Electron 30: 668-679.
- Buldu JM, Rogister F, Trull J, Serrat C, Torrent MC, et al. (2002) Asymmetric and delayed activation of side modes in multimode semiconductor lasers with optical feedback. Journal of Optics B: Quantum and Semiclassical Optics 4: 415-420.
- Yamada M, Huda M, Reraoka E, Kuwamura Y (2009) Effective noise reduction by electric positive and negative feedback in semiconductor lasers. IEEE Journal of Quantum Electron 45: 1248-1254.
- Stubkjaer K, Small MB (1983) Feedback-induced noise in index-guided semiconductor lasers and its reduction by modulation. Electronics Letters 19: 388-389.
- Gage EC, Beckens S (1990) Effects of high frequency injection and optical feedback on semiconductor laser performance. Proc. SPIE 1316: 199-204.
- Yamada M, Higashi T (1991) Mechanism of the noise reduction method by superposition of high-frequency current for semiconductor injection lasers. IEEE Journal of Quantum Electron 27: 380-388.
- Ohishi A, Chinone M, Ojima M, Arimoto A (1984) Noise characteristics of high-frequency superposed laser diodes for optical disc systems. Electronics Letters 20: 821-822.
- Matsui S, Takiguchi H, Hayashi H, Yamamoto S, Yano S, et al. (1983) Suppression of feedback-induced noise in short-cavity V-channelled substrate inner stripe lasers with self-oscillation Applied Physical Letter 43: 219-221.
- Yamada M (1996) Theoretical analysis of noise-reduction effect in semiconductor lasers with help of self-sustained pulsation phenomena. J. Appl. Phys. 79: 161-171.



12. Yamada M, Nakaya N, Funaki M (1987) Characteristics of mode-hopping noise and its suppression with the help of electric negative feedback in semiconductor lasers *IEEE J. Quantum Electron.* QE-23 8:1297-1302.
13. Agrawal GP, Dutta NK (1993) *Semiconductor Lasers*. VanNostrand Reinhold, New York.
14. Ahmed M, Yamada M (2010) Inducing single-mode oscillation in Fabry-PerotInGaAsP lasers by applying external optical feedback *IET. Optoelectronics* 4:133-141.
15. Ahmed M, Yamada M (2004) Field fluctuations and spectral line shape in semiconductor lasers subjected to optical feedback. *Journal of Applied Physics* 95:7573-7583.
16. Abdulrhman SG, Ahmed M, Okamoto T, Ishimori W, Yamada M (2003) An improved analysis of semiconductor laser dynamics under strong optical feedback. *Journal of selected topics in quantum electronics* 9: 1265-1274.
17. Ahmed M, Yamada M, Saito M (2001) Numerical modeling of intensity and phase noise in semiconductor lasers. *IEEE journal of quantum electronics* 37: 1600-1610.
18. Imran SMS, Yamada M, Kuwamura Y (2012) A theoretical analysis of the optical feedback noise based on multimode model of semiconductor lasers. *IEEE J. Quantum Electron* 48: 521-527.
19. Lang R, Kobayashi K (1980) External optical feedback effects on semiconductor injection laser properties. *IEEE J. Quantum Electron.* QE-16: 347-355.
20. Marcuse D (1984) Computer simulation of laser photon fluctuations: Theory of single cavity laser. *IEEE J. Quantum Electron* 20: 1139-1148.
21. Lasaosa D, Vega-Leal M, Fananas C (2008) Improved time-resolved simulation of amplitude and phase fluctuations in semiconductor laser light. *Journal of Opt. Quant. Electron* 40: 367-372.
22. Yamada M, Yamamura S, Okamoto T (2001) Characterization of the feedback induced noise in semiconductor lasers under superposition of high frequency current. *IEICE Trans. Electron.* E84-C 10.
23. Sacher J, Baums D, Panknin P, Elsässer W, Göbel EO (1992) Intensity instabilities of semiconductor lasers under current modulation, external light injection, and delayed feedback. *Phys Rev A* 45: 1893-1905.